Malaysian Journal of Chemistry, 2026, Vol. 28(1), 200-214
(Special Issue: *3rd International Conference on Industry-Academia Initiatives in Biotechnology & Chemistry, iCIABC2025*)

Development of Antibacterial Fish Gelatine/Carboxymethyl Cellulose Sugarcane Bagasse Blended Composite Film Reinforced ZnO Nanoparticles for Food Packaging

Siti Rodhiyah Sapie[1,2], Azlan Kamari[1]*, Siew Tin Susana Wong[1], Is Fatimah[3] and Saiful Irwan Zubairi[4]

[1]Department of Chemistry, Faculty of Science and Mathematics, Universiti Pendidikan Sultan Idris, 35900 Tanjong Malim, Perak, Malaysia

[2]Penang Matriculation College, Jalan Pongsu Seribu, 13200, Kepala Batas, Pulau Pinang, Malaysia

[3]Nanomaterials and Sustainable Chemistry Research Centre, Universitas Islam Indonesia, Chemistry Research Building, Kampus Terpadu UII, Jl. Kaliurang Km 14, Sleman, 55584, Yogyakarta, Indonesia

[4]Department of Food Sciences, Faculty of Science and Technology, Universiti Kebangsaan Malaysia, 43600 Bangi, Selangor, Malaysia

*Corresponding author (email: azlan.kamari@fsmt.upsi.edu.my)

Approximately 220 million metric tonnes of plastic wastes were produced in 2024, and this rises societal awareness regarding biodegradable and functional food packaging. Therefore, new antibacterial films were fabricated by blending fish gelatine (FG), carboxymethyl cellulose sugarcane bagasse (CMC SB), zinc oxide nanoparticles (ZnO NPs) and glycerol. The composite films were prepared at volume ratios of FG:CMC SB of 90:10, 70:30, and 50:50. Thickness, tensile strength (TS), elongation at break (EAB), water vapour permeability (WVP), oxygen permeability (OP) and surface morphology of biofilms were studied to assess the films' structural integrity and suitability. The antimicrobial activities were also evaluated against *Staphylococcus aureus* and *Escherichia coli*. Moreover, the fruit preservation efficacy of composite films was assessed under room temperature (27 °C) for 14 days. The addition of CMC SB and ZnO NPs significantly improved the TS and EAB of pure FG film by showing increments of 52.68% and 25.49%, respectively. The inhibition zone increased up to 1.80 cm (*S. aureus*) and 1.60 cm (*E. coli*). Overall, results from this work highlight the feasibility of composite films of FG/CMC SB reinforced with ZnO NPs as smart packaging films that can enhance the freshness and shelf life of food.

Keywords: Fish gelatine, carboxymethyl cellulose, zinc oxide nanoparticles, composite films, food packaging

Received: July 2025; Accepted: November 2025

Over the past decades, there has been a significant increase in global production and consumption of plastics. Approximately 40% of the global plastic waste originates from packaging. Petroleum-based plastics have been used for food packaging for over 75-80 years due to low production cost, ease of processing, and other excellent properties such as high moisture and gas barrier resistance, lightweight nature, flexibility, and durability [1, 2, 3]. However, these materials are not renewable and exhibit extremely low biodegradability, resulting in accumulation in plastic waste in the environment [4, 5]. Therefore, this industry currently has placed significant emphasis on sustainability and cost-saving measures.

Biodegradable plastics require higher production cost compared to traditional plastics. Hence, biopolymers, biodegradable polymers derived from biological sources, have been studied for their possible use in food packaging. Examples of biopolymers that have been explored are gelatine, starch, cellulose, tragacanth gum and so forth. This study focuses on the potential of fish gelatine and carboxymethyl cellulose (CMC) from sugarcane bagasse to be materials for food packaging. Gelatine is a biopolymer derived from collagen and is distinguished by its solubility in water and capacity to form thermally reversible gels [6]. Its broad application portfolio includes modern culinary techniques, biodegradable food packaging, cosmetic formulations, and drug delivery systems [7, 8, 9]. However, films cast from native gelatine exhibit reduced mechanical robustness when subjected to certain drying protocols; specifically, their elongation at break tends to be below 25%. Moreover, conventional single-layer gelatine membranes, characterised by periodic hydrophilic domains, are particularly vulnerable to moisture migration when in contact with high-water-content food matrices [10, 11]. Under these conditions, the films may undergo dissolution, dimensional swelling, or mechanical failure, compromising barrier integrity

†Paper presented at the 3rd International Conference on Industry-Academia Initiatives in Biotechnology & Chemistry

and functionality [12]. To address the shortcomings, suitable materials need to be added to pure gelatine. Luo et al. [13] identified several promising approaches to modify gelatine. These include blending gelatine with various natural polymers to enhance its mechanical properties, coupling gelatine with specific enzymes and proteins to tailor its functionality, incorporating phenolic compounds from plant sources to introduce antioxidant and antimicrobial traits, and embedding gelatine within nanomaterials to develop composites with improved barrier, structural, or release characteristics [14, 15, 16].

Agricultural waste generation has risen significantly, underscoring the pressing need for effective disposal and management approaches [17]. By transforming agricultural residues into biopolymers and other sustainable packaging matrices, waste decommissioning becomes aligned with environmental amelioration and economic valorisation. CMC, a polysaccharide of notable industrial importance, deployed traditionally as a gelling and thickening agent in food formulations. Its high solubility and enhanced viscometric properties render it a versatile component in immiscible blends for film formation. CMC is a potential substance for food packaging, providing advantages such as renewability, biodegradability, and excellent film-forming traits like clarity, durability, and moisture resistance. Pure CMC has several drawbacks including water sensitivity and inadequate UV protection, which leads to its common modification with other polymers or additives to improve its barrier, antioxidant, and antibacterial features for a more efficient and more eco-friendly substitute for traditional plastics [18].

Nanomaterials have attracted considerable attention in food packaging for their ability to enhance mechanical strength, barrier properties, and antimicrobial performance. Incorporating nanofillers such as nanoparticles, nanocrystals, and nanofibers into biopolymer matrices produces bio-nanocomposites with superior interfacial bonding and functionality [19, 20]. Among these, zinc oxide nanoparticles (ZnO NPs) stand out due to their thermal stability, mechanical reinforcement, and broad-spectrum antimicrobial activity. They are commercially available, non-toxic, and classified by the United States Food and Drug Administration (FDA) as generally recognised as safe (GRAS) for food-related uses [21]. ZnO NPs inhibit microbial growth by disrupting cell wall integrity and inducing oxidative stress, making them promising additives for active packaging.

Despite several research studies have developed nanomaterial-reinforced films, the information on FG and CMC SB as a blended matrix reinforced with ZnO NPs is scarce. The utilisation of CMC extracted from agro industrial by products not only promotes sustainable material valorisation but also enhances the physicochemical and functional properties of gelatine-based films. However, the combined effect of FG:CMC SB with ZnO NPs on the structural, mechanical, and antimicrobial performance of the resulting bionanocomposite films remains largely unexplored. Therefore, this study aims to address this research gap by developing and characterising FG:CMC–ZnO NPs composite films, highlighting their potential as sustainable and functional materials for active food packaging applications.

EXPERIMENTAL

Chemicals and Materials

Fish gelatine (FG) with bloom value of approximately 210 g and a mesh size of 20 was purchased from Halal Gelatin Hub, Malaysia. Carboxymethyl cellulose derived from sugarcane bagasse (CMC SB) was synthesised using the method described by Yaradoddi et al. [22] with minor modifications. Glycerol with a purity of ≥99.0% (GC), purchased from Sigma-Aldrich (Product No. G7757). The zinc oxide nanoparticles (ZnO NPs) were utilised in the as-received condition and did not undergo any additional purification procedures before experimentation. The nanoparticles were procured from Sigma-Aldrich with catalogue number of 721077. The supplied dispersion is characterised by a particle size distribution containing species with diameters less than 100 nm as observed by transmission electron microscopy (TEM), while the corresponding average diameter is determined to be 40 nm or less based on analytical particle sizing (APS) measurements.

Preparation of Films

In this study, the film preparation protocol was adapted from the methodology described by Khodaei et al. [23] with several deliberate modifications to improve film homogeneity, structural integrity, and nanoparticle dispersion. The ternary polymer blend of gelatine, tragacanth gum, and pectin reported in the original method was replaced with a binary composite comprising fish gelatine (FG) and carboxymethyl cellulose derived from sugarcane bagasse (CMC SB). Film-forming solutions (FFS) were formulated at FG:CMC SB ratios of 90:10, 70:30, and 50:50 (v/v), with the incorporation of zinc oxide nanoparticles (ZnO NPs) at a fixed concentration of 0.15 g, corresponding to approximately 2.5 wt% of the total polymer content. To ensure complete dissolution and remove residual insoluble matter, the CMC SB dispersion was centrifuged at 4,000 rpm for 10 min at 25 °C prior to blending. The resulting mixtures were then homogenised using an ultrasonic processor (500 W, 20 kHz, pulse mode: 11 s on/2 s off for 10 mins and subsequently degassed under vacuum for 20 mins to eliminate entrapped air bubbles. The films were cast into petri dishes and dried at 50 °C for 24 h, an

adjustment from the 30 °C drying temperature reported by Khodaei et al. [23] to promote uniform solvent evaporation and enhance film consistency.

Preparation of Fish Gelatine (FG) Solution

An exact 3.0 g of FG was initially suspended in 100 mL of deionised water and agitated in an IKA C-MAG HS 7 magnetic stirrer for 1 h at 750 revolutions per min. The suspension was then maintained at a constant temperature of 50 °C and stirred magnetically for another hour.

Preparation of Carboxymethyl Cellulose Sugarcane Bagasse (CMC SB) Solution

A 3.0 g mass of CMC SB was dispersed in 100 mL of deionised water. The resulting suspension was agitated with overhead stirring at ambient temperature for 1 h to ensure complete dissolution. The mixture was then centrifuged using a Hettich Rotofix 32A centrifuge at 4,000 rpm for 10 mins.

Preparation of FG:CMC SB Film Forming Solutions with ZnO NPs

Film-forming solutions (FFS) with different FG:CMC SB volume ratios, namely 90 FG:10 CMC SB, 70 FG:30 CMC SB, and 50 FG:50 CMC SB were prepared by mixing FG and CMC SB solutions. Subsequently, 1.5 mL of glycerol solution acts as a plasticiser was added to the mixture. Then, 0.15 g ZnO NPs was added to the mixture solution. Zinc oxide nanoparticles (ZnO NPs) were incorporated at a fixed amount of 0.15 g, corresponding to approximately 2.5 wt% relative to the total polymer weight and 0.15% (w/v) in the solution. The FFS was continuously stirred for another 1 h to ensure homogeneity. It was then homogenised using an Intelligent Ultrasonic Processor (Nanjing Genchen Scientific Instrument Co., Ltd.) equipped with a titanium probe operated at 500 W and 20 kHz in pulse mode. The mode was set active for 11 s and set pause for 2 s in a repeated cycle, continuing for a total duration of 10 mins to prevent overheating and ensure uniform dispersion of the nanofillers. The FFS samples were degassed under reduced pressure using a vacuum desiccator for 20 mins to remove dissolved gases. Pure gelatine films and 90 FG:10 CMC SB, 70 FG:30 CMC SB, and 50 FG:50 CMC SB without the addition of ZnO NPs were also prepared as controls.

Casting

Each aliquot (20 mL) of the FFS was pipetted and transferred with precision into 150 mL petri dish. The petri dishes containing the solution were then subjected to an isothermal treatment at 50 ºC for 24 h in a forced convection oven. Subsequent to drying, the resulting transparent films were manually detached and placed in a desiccator to maintain their hygroscopic stability prior to subsequent characterisation.

Characterisation of Films

In this work, the physicochemical properties all biopolymer films were characterised. In addition, all analyses were performed in triplicates and the data were presented as means ± standard deviation (SD).

Thickness

A film specimen exhibiting continuous surfaces, uniform texture, and consistent nominal thickness was obtained and divested into strips measuring 80 mm in length and 15 mm in width. The thickness of each resultant strip was quantified employing an INSIZE Digital Caliper Measuring Tool 1108-150. To ascertain a statistically robust average, three discrete measurements were performed at arbitrarily chosen locations along the length of each strip.

Tensile Strength (TS) and Elongation at break (EAB) Analyses

Biopolymer films were cut into 50 mm × 10 mm strips and their thickness measured at five points to calculate the average cross-sectional area. Tensile strength (TS) and elongation at break (EAB) of the films were determined according to ASTM D822 Standard test (ASTM) using an Instron 5967 Universal Testing Machine with a 1 kN load cell, flat pneumatic grips set 30 mm apart and a 0.1 N preload. TS was calculated by dividing the peak force at break by the original cross-sectional area, and EAB was calculated as the percentage increase in gauge length from 30 mm to the length at which the film failed.

Water Vapour Permeability (WVP) and Oxygen Permeability (OP) Analyses

WVP and OP of biopolymer films are commonly analysed to determine their functionality as barrier materials in packaging applications. In this study, the WVP was determined according to ASTM E96-2016 method using the following equation:

$$\mathrm{WVP} = \frac{\mathrm{WVTR}}{\Delta \mathrm{p}} \times l \quad (1)$$

Where Δp represents partial pressure difference of water vapour between the two sides of the film, l represents thickness of the material, and the water vapour transmission rate (WVTR) was calculated according to the following formula:

$$\mathrm{WVTR} = \frac{\Delta \mathrm{m}}{\mathrm{t.A}} \quad (2)$$

Where Δm is the change in mass; t is time taken for the mass change occurred and A is exposed area of the film.

OP was determined using the Systech Illinois 8501 Oxygen Permeability Analyser based on a coulometric sensor-based method that conforms to ASTM D3985. The oxygen transmission rate (OTR) is recorded in $cm^3/m^2 \cdot day \cdot atm$, and oxygen permeability (OP) is calculated using the formula:

$$OP = \frac{OTR \times l}{\Delta p} \quad (3)$$

In this expression, OTR denotes the oxygen transmission rate, l represents the film thickness, and $\triangle p$ is the oxygen partial pressure (kPa) across the film.

Transparency Properties

By using an Agilent Cary 60 UV-Visible Spectrophotometer, the opacity of the samples was determined at 600 nm. The transparency of the samples was assessed. The films were analysed at wavelengths ranging from 200 to 800 nm. The opacity values were calculated based on a formula proposed by Han and Floros [24]:

$$\text{Transparency} = \frac{A_{600}}{x} \quad (4)$$

Where, A is the absorbance value at 600 nm and x is the thickness (mm) of film samples.

Morphology and Microstructures

The surface morphology of the synthesised biopolymer films was examined using Field Emission Scanning Electron Microscopy (FESEM) to observe the structural uniformity, porosity, and nanoparticle dispersion. Before imaging, the films were sputter-coated with a thin layer of gold and analysed using a Hitachi SU8020 FESEM operated at an accelerating voltage of 2.0 kV. The morphologies of the biopolymer films prepared from FG and CMC SB with embedded ZnO NPs were studied at 25,000× magnifications in order to assess film uniformity and to elucidate the dispersion and integration of ZnO NPs within the hybrid matrix.

Fourier Transform Infrared (FTIR) Spectroscopy

Chemical composition, intermolecular interactions, and resultant functional properties of the films were analysed employing a Thermo Nicolet 6700 Fourier Transform Infrared Spectrometer. Infrared spectra were procured across the 4000-400 cm^{-1} wavenumber range, utilising a spectral resolution of 4 cm^{-1} and integrating a total of 32 scans for each measurement.

Functional Characterisation of Multifunctional Films

Antimicrobial Activity

The antimicrobial properties of the film samples were assessed according to the protocol outlined by Riaz et al. [25]. The study utilised two common bacterial strains, namely the Gram-positive *Staphylococcus aureus,* and the Gram-negative *Escherichia coli*. Bacterial inoculate were prepared by serially diluting overnight cultures to achieve a final concentration of 10^4 CFU/mL. A 0.1 mL portion of this suspension was uniformly spread across the surface of freshly prepared nutrient agar plates. Circular discs of 12 mm diameter were cut aseptically from the film samples and subjected to ultraviolet sterilisation prior to introduction onto the agar. Each sterilised disc was carefully placed on the inoculated agar plates and incubated at 37 °C for 24 h.

Fruits Freshness Monitoring and Preservation Study

The preservation efficacy of biocomposite films was evaluated using climacteric fruit dokong (*Lansium domesticum* Corr.) and non-climacteric fruit strawberry (*Fragaria × ananassa*), which differ fundamentally in ripening physiology: climacteric fruits exhibit a postharvest surge in ethylene biosynthesis and respiration that can be mitigated by controlling ethylene exposure and temperature, whereas non-climacteric fruits do not ripen further and must be harvested at full maturity and stored under low temperature and high humidity to reduce spoilage. Uniformly sized fruits were randomly selected, weighed, wrapped in the biocomposite films, and stored at room temperature (27 °C), with observations at 0, 7, and 14 days.

RESULTS AND DISCUSSION

Characterisation of Films

Mechanical Properties

Film thickness was measured before mechanical testing and the data were reported in Table 1. The neat FG film had an average thickness of 0.12 ± 0.0102 mm; blending with CMC SB resulted in incremental increases to 0.13 ± 0.0102 mm, 0.14 ± 0.0063 mm, and 0.14 ± 0.0049 mm for FG:CMC SB ratios of 90:10, 70:30, and 50:50, respectively. Addition of 0.15 g ZnO nanoparticles further elevated thickness to 0.17 ± 0.0075 mm, 0.18 ± 0.0098 mm, and 0.20 ± 0.0075 mm for the same blend compositions. These thickness values were employed to normalise tensile results, permitting valid comparisons of mechanical behaviour across samples. The observed increases indicate that both CMC SB and ZnO NPs act as effective fillers, promoting polymer–particle interactions, in agreement with observations by Yoo and Krochta [26] who reported a significant increase in thickness of whey protein–polysaccharide films following the addition of pure methycellulose (MC), hydroxypropylmethylcellulose (HPMC) and sodium alginate (SA).

The mechanical performance of FG:CMC SB blends is significantly improved by adding 0.15 g of

ZnO NPs; TS increased by 15-45% and EAB improved by 10-15% for all FG:CMC SB ratios. For instance, the 70:30 blend's elongation rose from 42.50 ± 2.95% to 48.24 ± 1.69%, and its tensile strength increased from 16.05 ± 1.90 MPa to 23.33 ± 1.52 MPa. Vyas et al. [27] observed a similar reinforcement effect in unmodified CMC/ZnO composites, reporting a tensile strength of 14.03 MPa and an elongation at break of 27.59% when ZnO was added at 20 wt%. The authors attributed these improvements to a homogeneous dispersion of ZnO nanoparticles and stronger polymer–filler interfacial bonding. Furthermore, Das et al. [28] found that solvent-cast chitosan films loaded with 2 to 6 wt% ZnO nanoparticles reached a peak increase in tensile strength of 133% at 4 wt% ZnO, accompanied by a noticeable rise in film thickness.

Incorporation of ZnO nanoparticles into FG: CMC SB film-forming systems produced a pronounced rise in dispersion viscosity, which translated into greater film thickness following solvent casting and drying. The viscosity augmentation is attributed to the increase in hydrogen-bonding and electrostatic interactions between the nanoparticulate surfaces and the polymer chains, promoting a tighter three-dimensional network that retains more solvent and swells during dehydration. Ultrasonic processing used to improve nanoparticle dispersion further modifies the rheological behaviour, producing more homogeneous suspensions and consequently films with improved uniformity and slightly larger bulk. Concurrent improvements in tensile strength and thermal resistance correlate with this structural reinforcement and help explain the observed increase in film thickness.

In a detailed study, Zafar et al. [29] conducted a comprehensive evaluation of how incremental ZnO nanoparticle loadings (1.0 to 2.5 wt%) affected the morphology and mechanical performance of carboxymethyl cellulose/gelatin hydrogel films. At the highest nanoparticle content (2.5 wt%), film thickness rose from 75 ± 2 µm for the unfilled CMC/GEL to 125 ± 3 µm. The authors explained that this was due to increment at dispersion viscosity and greater network swelling driven by the particles duolvent removal [30]. Incorporation of 1.5 wt% ZnO produced a substantial increase in tensile strength, from 14.6 ± 0.8 MPa for the neat film to 19.3 ± 1.0 MPa (≈32% improvement). Strength gains peaked near this loading level, with additional ZnO causing a plateau in mechanical performance consistent with the onset of nanoparticle agglomeration. The enhanced tensile strength and elongation at break exhibited by the film with a 70:30 FG:CMC SB composition containing ZnO nanoparticles likely resulted from an optimal interplay between polymer–polymer cohesion and polymer–nanoparticle interfacial bonding, which together provide effective stress transfer and maintain matrix flexibility [28]. At this ratio, the flexible gelatine matrix and the more rigid, hydrogen-bond-rich CMC SB phase complement each other, promoting strong interfacial adhesion and the formation of a cohesive biopolymer network. According to Das et al. [28], inclusion of ZnO nanoparticles further improves compatibility by providing reactive surface sites that promote additional hydrogen-bonding and electrostatic interactions between the polymer phases. The resulting, well-balanced interaction network facilitates efficient load transfer across interfaces and reinforces the composite structure, yielding increases in both mechanical strength and material ductility.

Water Vapour Permeability (WVP) and Oxygen Permeability (OP) Analysis

As presented in Table 2, the incorporation of 0.15 g ZnO NPs into FG:CMC SB films has resulted in significant increase in WVP and OP relative to ZnO NPs free controls. Specifically, WVP increased from 1.49 ± 0.26 to 1.73 ± 0.35 g m^{-1} day^{-1} atm^{-1}, while OP rose from 1.22 ± 0.77 × 10^{-4} to 1.45 ± 0.48 × 10^{-4} cm^3 m^{-2} day^{-1} atm^{-1}. These enhancements are attributed to ZnO NPs aggregation disrupting the polymeric network, which weakens intermolecular hydrogen bonding and increases free volume, thereby facilitating gas diffusion. Metal-oxide nanoparticles also perturb polymer crystallinity and chain mobility, further modulating barrier properties in bionanocomposite systems [31].

Table 1. Mechanical properties of biocomposite films.

Films	Thickness (mm)	Tensile Strength (MPa)	Elongation at Break (%)
Pure FG	0.12 ± 0.0102	15.28 ± 1.02	38.44 ± 1.73
(90 FG:10 CMC SB)	0.13 ± 0.0102	15.47 ± 1.19	38.93 ± 2.66
(70 FG:30 CMC SB)	0.14 ± 0.0063	16.05 ± 1.90	42.50 ± 2.95
(50 FG:50 CMC SB)	0.14 ± 0.0049	16.79 ± 1.28	43.36 ± 2.17
(90 FG:10 CMC SB) + 0.15 g ZnO NPs	0.17 ± 0.0075	18.84 ± 1.43	44.60 ± 2.18
(70 FG:30 CMC SB) + 0.15 g ZnO NPs	0.18 ± 0.0098	23.33 ± 1.52	48.24 ± 1.69
(50 FG:50 CMC SB) + 0.15 g ZnO NPs	0.20 ± 0.0075	21.68 ± 1.86	45.83 ± 1.61

Previously, several studies were reported increments in WVP and OP. For example, Shankar et al. [32] reported the incorporation of 2.5 mM ZnO NPs into the gelatine matrix slightly increased the WVP of the films from $1.25 \pm 0.12 \times 10^{-9}$ to $2.21 \pm 0.09 \times 10^{-9}$ g m m^{-2} $Pa^{-1}s^{-1}$. This is likely due to the formation of a more porous structure caused by the discontinuous distribution of nanoparticles within the polymer matrix. Lee et al. [33] found that the incorporation of 5% ZnO NPs into chicken skin gelatine/tapioca starch film enhanced the film's permeability by showing the WVP increment from 1.52 ± 0.11 x 10^{-7} g mm cm^{-2} h^{-1} Pa^{-1} to 1.93 ± 0.03 x 10^{-7} g mm cm^{-2} h^{-1} Pa^{-1}. The increase in WVP observed in this study may be ascribed to the non-uniform dispersion of nanoparticles within the bionanocomposite matrix, leading to nanoparticle aggregation and the formation of localized voids that facilitate moisture transmission. Similar observations were reported by Li et al. [34], marginal increase in WVP was observed with higher ZnO concentrations indicated that a decline in the film's resistance to water vapour transmission. The WVP rose from 0.0127 g m^{-1} h^{-1} Pa^{-1} for the control to 0.0157 g m^{-1} h^{-1} Pa^{-1} for the film containing 20% ZnO. This trend suggests that the incorporation of ZnO nanoparticles slightly disrupted the integrity of the starch matrix, possibly due to partial agglomeration or weak interfacial adhesion between the nanoparticles and polymer chains. Such micro-structural alterations may have facilitated easier diffusion of water vapour through the film, thereby slightly diminishing its barrier efficiency.

Although the incorporation of ZnO NPs resulted in increased WVP and OP values, these levels remain acceptable for certain food applications requiring moderate permeability. The increased permeability is likely attributed to the plasticising effect and enhanced polymer chain mobility introduced by ZnO NPs [35]. For fresh products like fruits and vegetables, packaging films with higher moisture and gas exchange rates are advantageous, as they help regulate respiration and prevent anaerobic conditions. In contrast, bakery items require low oxygen environments to reduce condensation and microbial spoilage [31]. Thus, although the elevated permeability may limit the films' suitability for highly sensitive products, they remain promising for applications where controlled respiration is essential to preserve freshness and extend shelf life. This highlights their potential in specific food sectors that demand partial permeability.

Table 2. WVP and OP values of biocomposite films.

Films	WVP (g m^{-1} day^{-1} atm^{-1})	OP $\times 10^{-4}$ (cm^3 m^{-2} day^{-1} atm^{-1})
Pure FG	1.56 ± 0.64	1.28 ± 0.30
(90 FG:10 CMC SB)	1.49 ± 0.26	1.22 ± 0.77
(70 FG:30 CMC SB)	1.35 ± 0.80	1.10 ± 0.54
(50 FG:50 CMC SB)	1.26 ± 0.32	1.01 ± 0.75
(90 FG:10 CMC SB) + 0.15 g ZnO NPs	1.73 ± 0.35	1.45 ± 0.48
(70 FG:30 CMC SB) + 0.15 g ZnO NPs	1.68 ± 0.98	1.31 ± 0.29
(50 FG:50 CMC SB) + 0.15 g ZnO NPs	1.55 ± 0.50	1.30 ± 0.65

Table 3. Light transmission and transparency of biocomposite films.

Films	Light transmission (%) at different wavelength							Transparency
	200 nm	280 nm	350 nm	400 nm	500 nm	600 nm	800 nm	
Pure FG	0.71	0.72	14.52	36.74	68.92	79.40	87.60	0.66
90 FG:10 CMC SB	1.32	2.84	18.42	44.26	69.20	79.32	88.50	0.61
70 FG:30 CMC SB	0.80	0.18	17.53	38.78	64.92	75.40	84.30	0.54
50 FG:50 CMC SB	0.72	1.48	14.92	34.66	58.20	71.68	78.96	0.51
90 FG:10 CMC SB + 0.15 g ZnO NPs	0.03	1.26	12.06	24.45	49.77	73.20	69.21	0.43
70 FG:30 CMC SB + 0.15 g ZnO NPs	0.02	1.08	10.62	23.11	45.33	68.56	68.32	0.38
50 FG:50 CMC SB + 0.15 g ZnO NPs	0.02	1.04	8.33	20.02	41.70	62.80	61.24	0.31

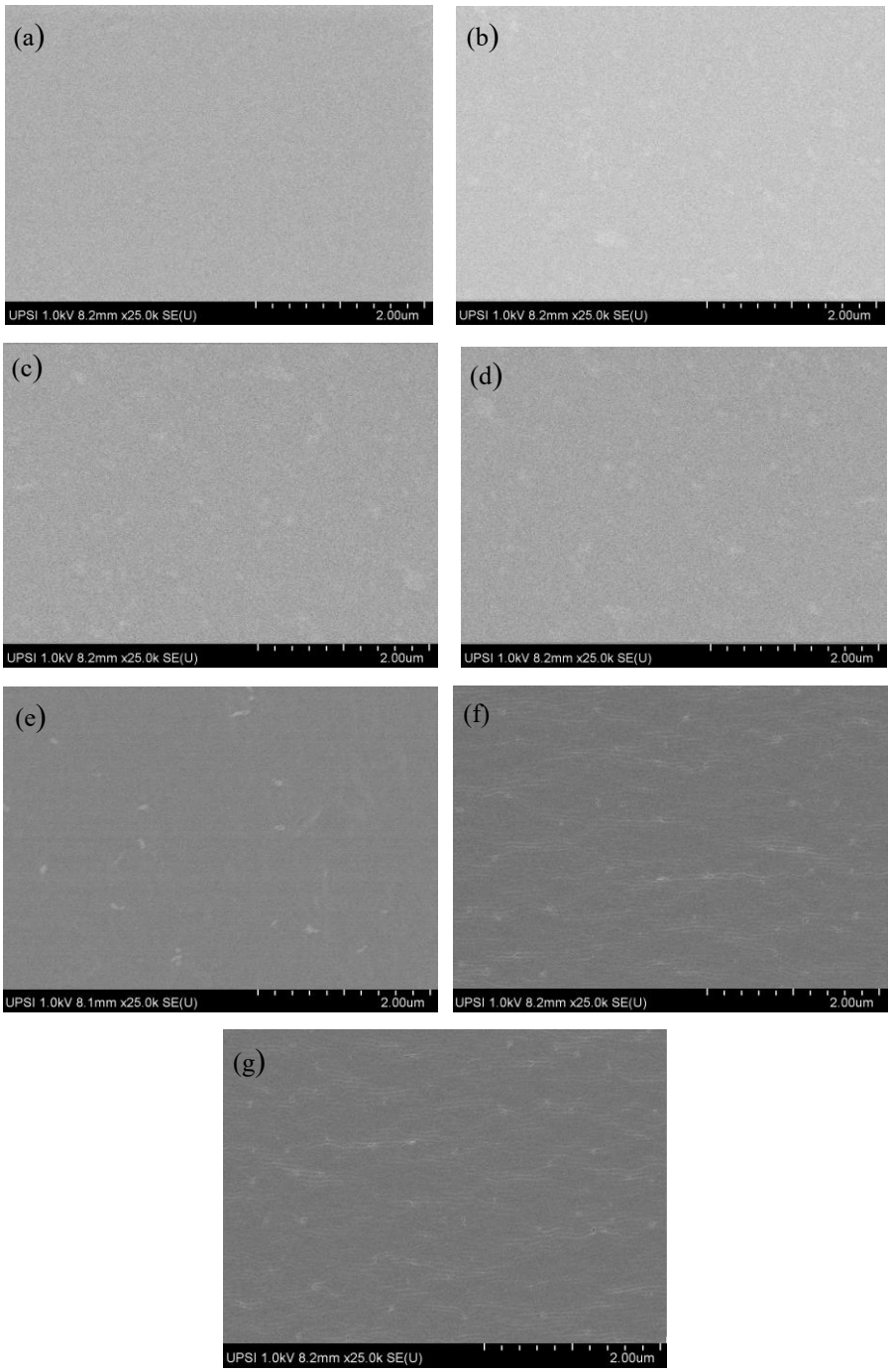

Figure 1. FESEM images of (a) Pure FG, (b) 90 FG:10 CMC SB , (c) 70 FG:30 CMC SB, (d) 50 FG:50 CMC SB, (e) 90 FG:10 CMC SB + 0.15 g ZnO NPs, (f) 70 FG:30 CMC SB + 0.15 g ZnO NPs, and (g) 50 FG:50 CMC SB + 0.15 g ZnO NPs at 25,000× magnification

Transparency Properties

The studies on light transmission and transparency properties are inevitable in such development of films for food packaging. From Table 3, the transparency measurements of FG films revealed a clear, concentration dependent decline in light transmittance: pure FG exhibited a value of 0.66, which decreased to 0.61, 0.54 and 0.51 upon incorporation of 10, 30 and 50% CMC SB, respectively, and dropped further to 0.43, 0.38 and 0.31 when ZnO NPs were included in those same FG:CMC SB matrices. This optical attenuation is first attributed to CMC SB-induced disruption of the gelatine network and formation of additional amorphous microdomains that scatter incident light, and second to the well-documented light-absorbing and scattering effects of ZnO NPs within heterogeneous [34]. Functionally, the resulting opacity enhances ultraviolet–visible barrier performance, thereby retarding photochemical oxidation of sensitive nutrients and pigments and extending the shelf life of light-vulnerable foods such

as oils, dairy products, and seafood. The inherent antibacterial properties of ZnO confer active protection to the biocomposite films, inhibiting microbial proliferation and lowering the likelihood of food spoilage. Moreover, the intrinsic antimicrobial activity of ZnO transforms these composites into active packaging materials capable of suppressing microbial growth and reducing spoilage risk [35]. Coupled with the adjustable optical clarity of FG:CMC SB matrices reinforced with ZnO nanoparticles, these materials are well suited as biodegradable, multifunctional coatings for safeguarding light- sensitive food products.

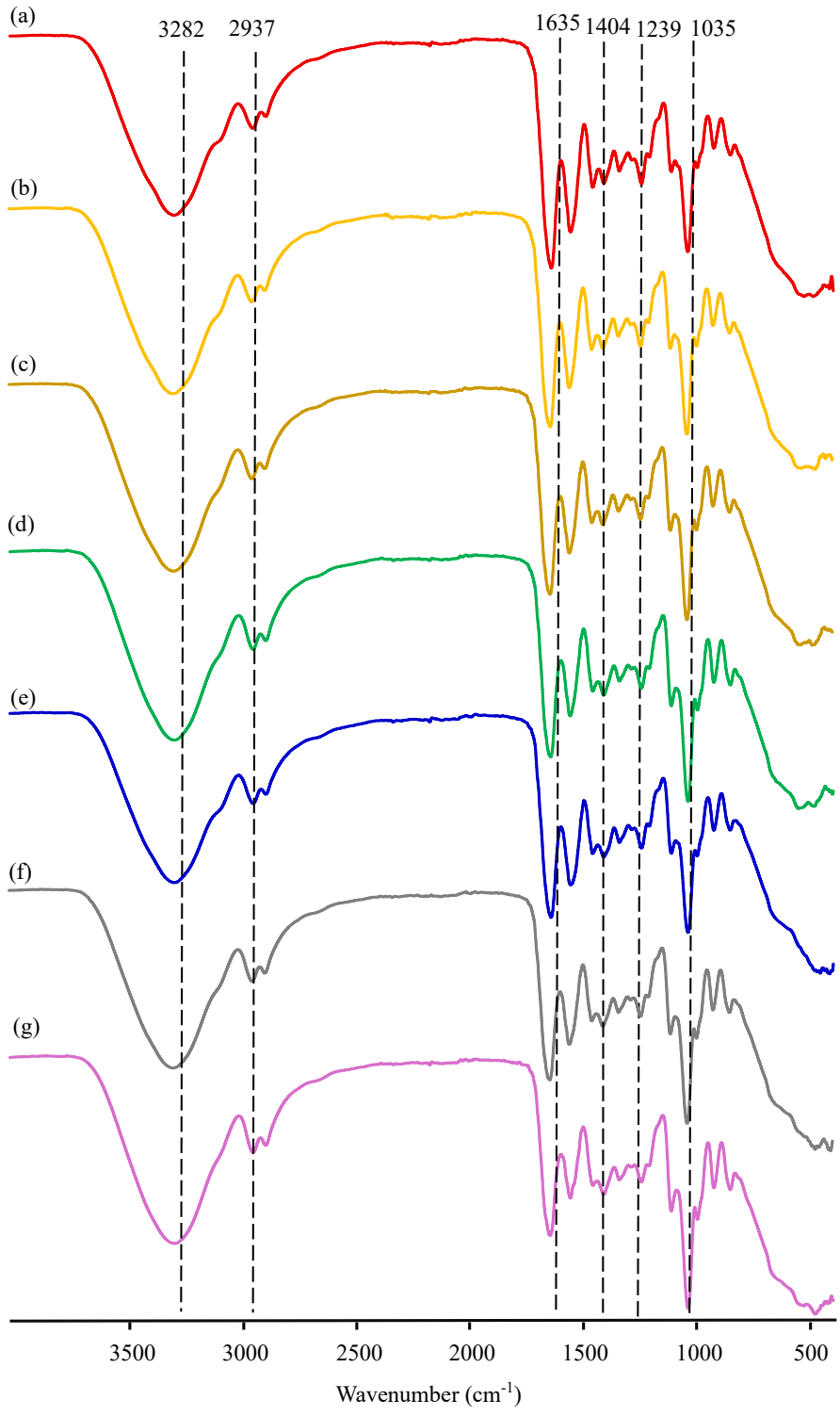

Figure 2. FTIR spectra of (a) pure FG, (b) 90 FG:10 CMC SB, (c) 70 FG:30 CMC SB, (d) 50 FG:50 CMC SB, (e) 90 FG:10 CMC SB + 0.15 g ZnO NPs, (f) 70 FG:30 CMC SB + 0.15 g ZnO NPs, and (g) 50 FG:50 CMC SB + 0.15 g ZnO NPs films.

Morphology and Microstructures

FESEM was employed to examine the films' microstructure. The representative micrographs of biocomposite films at 25,000× are shown in Figure 1. As can be seen from Figure 1(a), pure FG film exhibited a largely featureless, continuous surface with only occasional pores and no visible fissures, indicative of a compact, homogeneous matrix. This finding corroborated with the results of Ratna et al [36]. Progressive addition of CMC SB altered surface morphology: the 90:10 FG:CMC SB blend displayed sparse microvoids and slight roughening (Figure 1(b)), the 70:30 blend showed emerging phase boundaries and the onset of microfibrillar features (Figure 1(c)), and the 50:50 formulation revealed pronounced phase separation and notable topographical heterogeneity (Figure 1(d)), suggesting reduced miscibility between components. Introduction of ZnO nanoparticles produced near-spherical particles well embedded in the 90:10 matrix (Figure 1(e)), whereas the 70:30 system exhibited moderate particle aggregation (Figure 1(f)) and the 50:50 system showed extensive nanoparticle clustering (Figure 1(g)), trends that coincide with increasing surface texturing and stronger particle–polymer interfacial effects [37]. The observed changes in surface morphology reflect differences in nanoparticle distribution and polymer miscibility among the formulations, demonstrating that both blend composition and ZnO loading substantially affect the films' microstructural coherence and integrity.

FTIR Analysis

The interactions between the FG:CMC SB matrix and ZnO nanoparticles were evaluated by FTIR, with spectra recorded across 4000 to 400 cm^{-1} range (Figure 2). All samples showed the expected absorption features associated with the constituent biopolymer functional groups.

The broad band near 3282 cm^{-1} corresponded to O–H stretching and amide A (N–H) vibrations. In the FG:CMC SB blends this band broadens and shifts marginally to lower wavenumbers, consistent with strengthened hydrogen-bonding between the hydroxyl groups of CMC SB and the amino/hydroxyl moieties of gelatine [38-44]. The incorporation of ZnO NPs further broadens this band, suggesting possible coordination interactions between Zn^{2+} ions or surface hydroxyls of ZnO and the polar functional groups (–OH, –NH) in the polymer chains [45]. Similar shifts have been reported in gelatine-based or polysaccharide-based nanocomposites containing ZnO, confirming strong polymer–nanoparticle hydrogen bonding [46]. The band at 2937 cm^{-1} was corresponding to C–H stretching vibrations of aliphatic groups and it remains relatively stable, indicating that the backbone structure of the polymer matrix is not significantly altered by blending or nanoparticle addition. The amide I band, located at the region between 1633 and 1635 cm^{-1}, is associated with C=O stretching vibrations of peptide linkages. Slight shifts and intensity variations observed with increasing CMC SB content suggest changes in the protein secondary structure and possible electrostatic interactions between carboxyl groups of CMC SB and amino groups of gelatine [47]. The peaks around 1404 cm^{-1} (C–N stretching or COO^- symmetric stretching) and 1239 cm^{-1} (amide III or C–O–C stretching) increase in intensity in ZnO-containing films, indicating the formation of coordination or complexation interactions between Zn^{2+} and oxygen-containing functional groups within the matrix [48, 49]. The 1035 cm^{-1} band, attributed to C–O–C and C–O stretching vibrations in the polysaccharide backbone, exhibits a slight shift and intensity enhancement upon ZnO incorporation, consistent with strong polymer–nanoparticle interactions and improved interfacial compatibility [50]. Additionally, the appearance or intensification of absorption bands in the 500–700 cm^{-1} region corresponds to the Zn–O stretching vibration, confirming the presence and successful incorporation of ZnO NPs within the FG:CMC SB network [51]. Overall, these spectral modifications confirm the establishment of intermolecular interactions, particularly hydrogen bonding and Zn^{2+} coordination between FG, CMC SB, and ZnO NPs, signifying good interfacial adhesion and homogeneous nanoparticle dispersion in the biopolymer composite.

Functional Characterisation of Multifunctional Films

Antimicrobial Activity

As shown in Table 4, the incorporation of ZnO NPs into the FG:CMC films significantly enhanced antimicrobial performance against both *S. aureus* (Gram-positive) and *E. coli* (Gram-negative). This improvement is evidenced by a marked increase in the inhibition zone area compared to films without ZnO NPs, indicating the effective antibacterial action of the nanoparticles within the biocomposite matrix. When 0.15 g of ZnO NPs was present in FG:CMC films, clear inhibition zones were observed for both test organisms, with zone diameters increasing as the CMC SB proportion rose. For *S. aureus*, the inhibition expanded from 1.60 ± 0.42 cm for the 90:10 FG:CMC SB formulation to 1.80 ± 0.21 cm for the 50:50 blend. *E. coli* exhibited a corresponding increase from 1.30 ± 0.54 cm to 1.60 ± 0.25 cm across the same composition range, reflecting enhanced antimicrobial performance with greater CMC SB content [37].

The data indicated that both the polymer blend composition and the amount of ZnO nanoparticles jointly determine antimicrobial efficacy. Films containing ZnO showed stronger inhibition of *S. aureus* than of *E. coli*, a pattern that can be explained

by the protective outer membrane of Gram-negative bacteria which can hinder nanoparticle access, whereas Gram-positive organisms, with their more exposed peptidoglycan layer, are typically more vulnerable to nanoparticle-mediated antimicrobial action. The larger inhibition zones are explained by the antimicrobial action of ZnO nanoparticles, which promote formation of reactive oxygen species including hydroxyl radicals, superoxide anions, and hydrogen peroxide that damage microbial cells [37]. According to Jin and Jin [47], reactive oxygen species (ROS) generated by ZnO nanoparticles cause oxidative stress that damages key cellular components, producing membrane disruption, protein unfolding, and nucleic acid breakdown. In *E. coli* (Gram-negative), ZnO primarily compromises the outer membrane, increasing permeability and promoting leakage of intracellular contents. While in *S. aureus* (Gram-positive), ROS penetrate the thicker peptidoglycan layer and impair vital internal structures. The combined effects of oxidative damage and membrane destabilization hinder bacterial viability and produce larger inhibition zones [37].

The antimicrobial activity of ZnO nanoparticles operates through three complementary routes: generation of ROS, liberation of Zn^{2+} ions, and direct physical disruption of bacterial membranes via nanoparticle–cell contact. Incorporating ZnO into a CMC matrix increases the film's hydrophilicity and promotes an even nanoparticle dispersion, which helps sustain a controlled release gradient of Zn^{2+} and allows ROS to diffuse effectively through the film. An increase in exposed nanoparticle surface area amplifies ROS production and thus strengthens microbial inactivation [27].

Fruits Freshness Monitoring and Preservation Study

Visual appearance was used to evaluate the efficacy of FG:CMC SB films in extending the shelf life of both climacteric fruit, dokong (*Lansium domesticum* Corr.), and non-climacteric fruit, strawberry (*Fragaria* × *ananassa*), over a 14-day storage period, as shown in Figures 3 and 4. Unwrapped controls exhibited severe shrinkage and surface fungal growth, which intensified by day 14. In contrast, fruits wrapped in FG:CMC SB added with ZnO NPs films showed noticeable shrinkage but remained free of microbial infection throughout the test.

Biopolymer film, which covers the surface of fruits and vegetables and lowers the absolute value of air volume and air movement, is a significant packaging material that demonstrates effective preservation performance and satisfies requirements. Conversely, they served as barriers that obstruct the departure of water and carbon dioxide from fruits and vegetables as well as the admission of ambient oxygen. Though it is beneficial, the increased shelf life caused by the films is somewhat at odds with the characteristics of the fruits, and vegetables because they prevent degradation by slowing down the metabolic process of fruits and vegetables. The sodium alginate-coated film developed by Senturk Parreidt et al. [52] markedly decreased weight loss in cantaloupe and strawberries.

Table 4. Inhibition zone of biocomposite films against *S. aureus* and *E. coli*.

Films	Inhibition zone (cm)	
	S. aureus	***E. coli***
Commercial cling film	1.25 ± 0.23	1.31 ± 0.19
Pure FG	No inhibition	No inhibition
90 FG:10 CMC SB	No inhibition	No inhibition
70 FG:30 CMC SB	No inhibition	No inhibition
50 FG:50 CMC SB	No inhibition	No inhibition
90 FG:10 CMC SB + 0.15 g ZnO	1.60 ± 0.42	1.30 ± 0.54
70 FG:30 CMC SB + 0.15 g ZnO	1.70 ± 0.38	1.50 ± 0.46
50 FG:50 CMC SB + 0.15 g ZnO	1.80 ± 0.21	1.60 ± 0.25

Film Composition	Day 1	Day 7	Day 14
Unwrapped dokong (*Lansium domesticum* Corr.)			
Pure FG			
(90 FG: 10 CMC SB)			
(70 FG: 30 CMC SB)			
(50 FG: 50 CMC SB)			
(90 FG: 10 CMC SB) + 0.15 g ZnO			
(70 FG: 30 CMC SB) + 0.15 g ZnO			
(50 FG: 50 CMC SB) + 0.15 g ZnO			

Figure 3. The changes in visual appearance of dokong (*Lansium domesticum Corr*.), without any packaging or unwrapped and wrapped with biocomposite films over a period of 14 days

Films Composition	Day 1	Day 7	Day 14
Unwrapped strawberry (*Fragaria* × *ananassa*)			

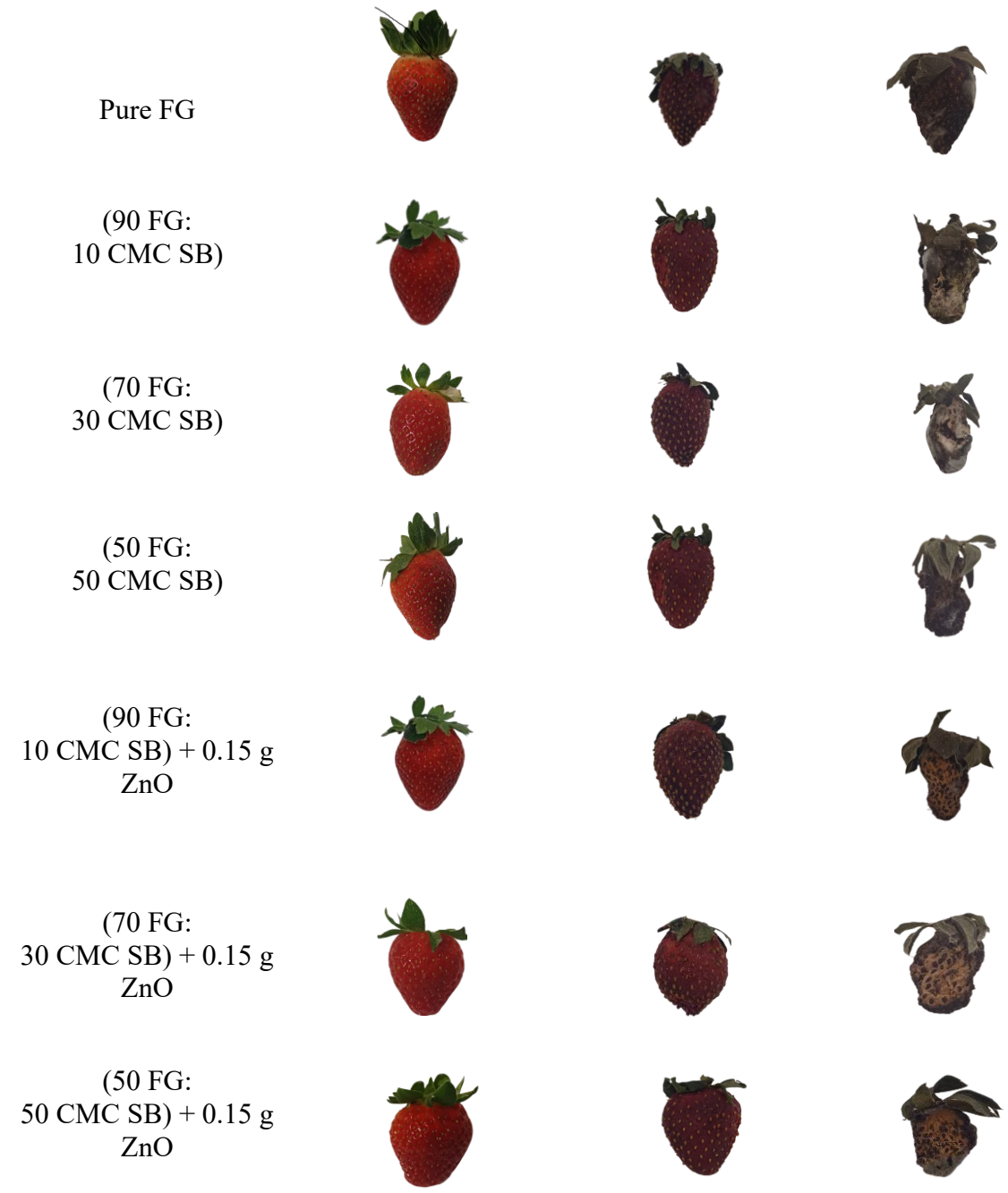

Figure 4. The changes in visual appearance of strawberry (*Fragaria* × *ananassa*), without any packaging or unwrapped and wrapped with biocomposite films over a period of 14 days

CONCLUSION

In summary, the overall aim of this study was successfully achieved with 70 FG:30 CMC SB was the optimum ratio for biofilm formulation. This ratio has improved the tensile strength (from 15.28 MPa to 23.33 MPa) and elongation at break (from 38.44% to 48.24%), respectively. Additionally, the antimicrobial inhibition zone increased up to 1.80 cm for *S. aureus* and 1.60 cm for *E. coli*. Although results from this study highlight the potential of gelatine-CMC based biofilms against *S. aureus* and *E. coli*, it would be interesting to evaluate the antimicrobial activity of these biofilms on other foodborne pathogens such as *Salmonella* and *Listeria* in the future research. The fruits were successfully preserved under room condition (27 °C) for 14 days with reduction in microbial spoilage. Based on obtained results, the effectiveness of biofilm incorporated with ZnO was in the order was 70 FG:30 CMC SB > 50 FG:50 CMC SB > 90 FG:10 CMC SB. Taking everything into account, antibacterial FG:CMC SB blended composite films reinforced ZnO NPs could be alternatives for preserving fruits, contributing to a more sustainable

and environmental-friendly food packaging industry. The FG:CMC SB:ZnO nanocomposite films present considerable promise as eco-conscious substitutes for conventional petroleum-derived packaging. Although their mechanical strength is somewhat inferior to synthetic polymers such as polyethylene and polypropylene, they retain sufficient flexibility and resilience for use in packaging perishable or short shelf-life food items. The incorporation of inexpensive, renewable, and abundantly available constituents enhances both the economic feasibility and environmental appeal of these materials. Furthermore, the straightforward solution casting technique is compatible with existing industrial film fabrication and coating processes, suggesting favourable prospects for scale-up. With continued refinement in composition and processing, these biopolymer-based films offer a compelling, biodegradable, and safe solution for sustainable food packaging applications.

ACKNOWLEDGEMENTS

Siti Rodhiyah Sapie thanks to Ministry of Education Malaysia for providing a PhD scholarship, Federal Training Prize Program (HLPS). The authors would like to express their sincere gratitude to the Nanotechnology Research Centre, Faculty of Science and Mathematics, Universiti Pendidikan Sultan Idris (UPSI) for providing the necessary research facilities and support throughout this study. Special thanks are also extended to Penang Matriculation College, Universitas Islam Indonesia and Universiti Kebangsaan Malaysia for their collaborative contributions and technical assistance.

REFERENCES

1. Ncube, L. K., Ude, A. U., Ogunmuyiwa, E. N., Zulkifli, R. and Beas, I. N. (2020) Environmental impact of food packaging materials: A review of contemporary development from conventional plastics to polylactic acid based materials. *Materials*, **13(21)**, 4994.

2. Hong, L. G., Yuhana, N. Y. and Zawawi, E. Z. E. (2021) Review of bioplastics as food packaging materials. *AIMS Materials Science*, **8(2)**, 166–184.

3. Yin, Y. and Woo, M. W. (2024) Transitioning of petroleum-based plastic food packaging to sustainable bio-based alternatives. *Sustainable Food Technology*, **2(3)**, 548–566.

4. Dirpan, A., Ainani, A. F. and Djalal, M. (2023) A review on biopolymer-based biodegradable film for food packaging: Trends over the last decade and future research. *Polymers*, **15(13)**, 2781.

5. Omer, S. S. and Hassan, N. E. (2024) Application of biodegradable plastic and their environmental impacts: A review. *World Journal of Advanced Research and Reviews*, **21(1)**, 2139–2148.

6. Ahmad, M. I., Li, Y., Pan, J., Liu, F., Dai, H., Fu, Y., Huang, T., Farooq, S. and Zhang, H. (2024) Collagen and gelatin: Structure, properties, and applications in food industry. *International Journal of Biological Macromolecules*, **254**, 128037.

7. Rathod, N. B., Bangar, S. P., Šimat, V. and Ozogul, F. (2023) Chitosan and gelatine biopolymer-based active/biodegradable packaging for the preservation of fish and fishery products. *International Journal of Food Science and Technology*, **58(2)**, 854–861.

8. Alipal, J., Pu'Ad, N. M., Lee, T. C., Nayan, N. H. M., Sahari, N., Basri, H., Idris, M. I. and Abdullah, H. Z. (2021) A review of gelatin: Properties, sources, process, applications, and commercialization. *Materials Today: Proceedings*, **42**, 240–250.

9. Lu, Y., Luo, Q., Chu, Y., Tao, N., Deng, S., Wang, L. and Li, L. (2022) Application of gelatin in food packaging: A review. *Polymers*, **14(3)**, 436.

10. Xu, X., Xi, Y. and Weng, Y. (2025) Gelatin-based materials: fabrication, properties and applications in the food packaging system. *RSC advances*, **15(37)**, 30605–30621.

11. Reji, R. E., Mathew, C. B., Sabu, C. S. and Roy, S. (2025) A review on gelatin films and coatings for active food packaging: functional properties and applications. *Food Innovation and Advances*, **4(3)**, 423–436.

12. Kulalı Gül, M. and Turkmen, H. (2025) Improvement of gelatin-based coating in order to enhance the oxygen barrier and mechanical properties of biobased PLA (polylactic acid) and cellulose films. *ACS Omega*, **10(29)**, 31401–31409.

13. Luo, Q., Hossen, M. A., Zeng, Y., Dai, J., Li, S., Qin, W. and Liu, Y. (2022) Gelatin-based composite films and their application in food packaging: A review. *Journal of Food Engineering*, **313**, 110762.

14. Derkach, S. R., Voron'ko, N. G., Kuchina, Y. A. and Kolotova, D. S. (2020) Modified fish gelatin as an alternative to mammalian gelatin in modern food technologies. *Polymers*, **12(12)**, 3051.

15. Joy, J. M., Padmaprakashan, A., Pradeep, A., Paul, P. T., Mannuthy, R. J. and Mathew, S. (2024) A review on fish skin-derived gelatin: elucidating the gelatin peptides—preparation,

bioactivity, mechanistic insights, and strategies for stability improvement. *Foods*, **13(17)**, 2793.

16. Gubaidullin, A. T., Galeeva, A. I., Galyametdinov, Y. G., Ageev, G. G., Piryazev, A. A., Ivanov, D. A., Ermakova, E. A., Nikiforova, A. A., Derkach, S. R., Zueva, O. S. and Zuev, Y. F. (2025) Modulation of Structural and Physical-Chemical Properties of Fish Gelatin Hydrogel by Natural Polysaccharides. *International Journal of Molecular Sciences*, **26(7)**, 2901.

17 Homsaard, N., Kodsangma, A., Jantrawut, P., Rachtanapun, P., Leksawasdi, N., Phimolsiripol, Y., Seesuriyachan, P., Chaiyaso, T., Sommano, S. R., Rohindra, D. and Jantanasakulwong, K. (2021) Efficacy of cassava starch blending with gelling agents and palm oil coating in improving egg shelf life. *International Journal of Food Science and Technology*, **56(8)**, 3655–3661.

18. Sharma, C., Kundu, S., Singh, S., Saxena, J., Gautam, S., Kumar, A. and Pathak, P. (2025) From concept to shelf: engineering biopolymer-based food packaging for sustainability. *RSC Sustainability*, **3**, 4992–5026.

19. Pal, K., Sarkar, P., Anis, A., Wiszumirska, K. and Jarzębski, M. (2021) Polysaccharide-based nanocomposites for food packaging applications. *Materials*, **14(19)**, 5549.

20. Pires, J. R. A., Rodrigues, C., Coelhoso, I., Fernando, A. L. and Souza, V. G. L. (2023) Current applications of bionanocomposites in food processing and packaging. *Polymers*, **15(10)**, 2336.

21. Youn, S. M. and Choi, S. J. (2022) Food additive zinc oxide nanoparticles: dissolution, interaction, fate, cytotoxicity, and oral toxicity. *International Journal of Molecular Sciences*, **23(11)**, 6074.

22. Yaradoddi, J. S., Banapurmath, N. R., Ganachari, S. V., Soudagar, M. E. M., Mubarak, N. M., Hallad, S., Hugar, S. and Fayaz, H. (2020) Biodegradable carboxymethyl cellulose based material for sustainable packaging application. *Scientific Reports*, **10(1)**, 21960.

23. Khodaei, D., Oltrogge, K. and Hamidi-Esfahani, Z. (2020) Preparation and characterization of blended edible films manufactured using gelatin, tragacanth gum and, Persian gum. *LWT*, **117**, 108617.

24. Han, J. H. and Floros, J. D. (1997) Casting antimicrobial packaging films and measuring their physical properties and antimicrobial activity. *Journal of Plastic Film and Sheeting*, **13(4)**, 287–298.

25. Riaz, A., Lagnika, C., Luo, H., Dai, Z., Nie, M., Hashim, M. M., Liu, C., Song, J. and Li, D. (2020) Chitosan-based biodegradable active food packaging film containing Chinese chive (*Allium tuberosum*) root extract for food application. *International Journal of Biological Macromolecules*, **150**, 595–604.

26. Yoo, S. and Krochta, J. M. (2011) Whey protein–polysaccharide blended edible film formation and barrier, tensile, thermal and transparency properties. *Journal of the Science of Food and Agriculture*, **91(14)**, 2628–2636.

27. Vyas, A., Ng, S. P., Fu, T. and Anum, I. (2025) A facile preparation and characterization of a sustainable and superhydrophobic carboxymethyl cellulose/ZnO composite film. *Cellulose*, **32(6)**, 3833–3853.

28. Das, K., Maiti, S. and Liu, D. (2014) Morphological, mechanical and thermal study of ZnO nanoparticle reinforced chitosan based transparent biocomposite films. *Journal of The Institution of Engineers (India): Series D*, **95(1)**, 35–41.

29. Zafar, A., Khosa, M. K., Noor, A., Qayyum, S. and Saif, M. J. (2022) Carboxymethyl cellulose /gelatin hydrogel films loaded with zinc oxide nanoparticles for sustainable food packaging applications. *Polymers*, **14(23)**, 5201.

30. Hanemann, T. and Szabó, D. V. (2010) Polymer-nanoparticle composites: from synthesis to modern applications. *Materials*, **3(6)**, 3468–3517.

31. Sorrentino, A., Gorrasi, G. and Vittoria, V. (2007) Potential perspectives of bio-nanocomposites for food packaging applications. *Trends in Food Science and Technology*, **18(2)**, 84–95.

32. Shankar, S., Teng, X. and Rhim, J. W. (2014) Effects of concentration of ZnO nanoparticles on mechanical, optical, thermal, and antimicrobial properties of gelatin/ZnO nanocomposite films. *Korean Journal of Packaging Science and Technology*, **20**, 41–49.

33. Lee, S. W., Said, N. S. and Sarbon, N. M. (2021) The effects of zinc oxide nanoparticles on the physical, mechanical, and antimicrobial properties of chicken skin gelatin/tapioca starch composite films in food packaging. *Journal of Food Science and Technology*, **58(11)**, 4294–4302.

34. Li, L., Chin, S. X., Rachtanapun, P., Amornsakchai, T., Khiew, P., Chowdhury, S., Zakaria, S. and Chia, C. H. (2025) Cellulose nanocrystals and zinc oxide in pineapple starch films for enhanced banana shelf-life. *Sains Malaysiana*, **54(3)**, 899–911.

35. Arfat, Y. A., Benjakul, S., Prodpran, T., Sumpavapol, P. and Songtipya, P. (2016) Physico-mechanical characterization and antimicrobial properties of fish protein isolate/fish skin gelatin-zinc oxide (ZnO) nanocomposite films. *Food and Bioprocess Technology*, **9(1)**, 101–112.

36. Ratna, Aprilia, S., Arahman, N., Bilad, M. R., Suhaimi, H., Munawar, A. A. and Nasution, I. S. (2022) Bio-nanocomposite based on edible gelatin film as active packaging from *Clarias gariepinus* fish skin with the addition of cellulose nanocrystalline and nanopropolis. *Polymers*, **14(18)**, 3738.

37. Sultan, M., Ibrahim, H., El-Masry, H. M. and Hassan, Y. R. (2024) Antimicrobial gelatin-based films with cinnamaldehyde and ZnO nanoparticles for sustainable food packaging. *Scientific Reports*, **14(1)**, 22499.

38. Gómez-Guillén, M. C., Giménez, B., López-Caballero, M. A. and Montero, M. P. (2011) Functional and bioactive properties of collagen and gelatin from alternative sources: A review. *Food Hydrocolloids*, **25(8)**, 1813–1827.

39. Vafaei, E., Hasani, M., Salehi, N., Sabbagh, F. and Hasani, S. (2025) Enhancement of biopolymer film properties using spermidine, zinc oxide, and graphene oxide nanoparticles: A study of physical, thermal, and mechanical characteristics. *Materials*, **18(2)**, 225.

40. Hosseini, S. F., Rezaei, M., Zandi, M. and Farahmandghavi, F. (2016) Development of bioactive fish gelatin/chitosan nanoparticles composite films with antimicrobial properties. *Food Chemistry*, **194**, 1266–1274.

41. Badry, R., Sabry, N. M. and Ibrahim, M. A. (2024) Enhancing the structural and optoelectronic properties of carboxymethyl cellulose sodium filled with ZnO/GO and CuO/GO nanocomposites for antimicrobial packaging applications. *Scientific Reports*, **14(1)**, 30591.

42. Abdollahi, M., Rezaei, M. and Farzi, G. (2012) Improvement of active chitosan film properties with rosemary essential oil for food packaging. *International Journal of Food Science and Technology*, **47(4)**, 847–853.

43. Al-Naamani, L., Dutta, J. and Dobretsov, S. (2018) Nanocomposite zinc oxide-chitosan coatings on polyethylene films for extending storage life of okra (*Abelmoschus esculentus*). *Nanomaterials*, **8(7)**, 479.

44. Kanmani, P. and Rhim, J. W. (2014) Physical, mechanical and antimicrobial properties of gelatin based active nanocomposite films containing AgNPs and nanoclay. *Food Hydrocolloids*, **35**, 644–652.

45. Mobarraei, M., Babaei, S., Naseri, M., Esmaeili, M. and Moosavi-Nasab, M. (2025) Effect of zinc oxide nanoparticles on the physical, mechanical, and antibacterial properties of active packaging films based on *Gracilaria corticata* agar and fish skin gelatin. *Food and Bioprocess Technology*, **18**, 8055–8070.

46. Nan, J., Chu, Y., Guo, R. and Chen, P. (2024) Research on the antibacterial properties of nanoscale zinc oxide particles comprehensive review. *Frontiers in Materials*, **11**, 1449614.

47. Jin, S. E. and Jin, H. E. (2021) Antimicrobial activity of zinc oxide nano/microparticles and their combinations against pathogenic microorganisms for biomedical applications: From physicochemical characteristics to pharmacological aspects. *Nanomaterials*, **11(2)**, 263.

48. Mendes, A. R., Granadeiro, C. M., Leite, A., Pereira, E., Teixeira, P. and Poças, F. (2024) Optimizing antimicrobial efficacy: Investigating the impact of zinc oxide nanoparticle shape and size. *Nanomaterials*, **14(7)**, 638.

49. Abdullah, J. A. A., Jiménez-Rosado, M., Guerrero, A. and Romero, A. (2022) Biopolymer-based films reinforced with green synthesized zinc oxide nanoparticles. *Polymers*, **14(23)**, 5202.

50. Voorhis, C., González-Benito, J. and Kramar, A. (2024) "Nano in Nano"—Incorporation of ZnO Nanoparticles into Cellulose Acetate–Poly (Ethylene Oxide) Composite Nanofibers Using Solution Blow Spinning. *Polymers*, **16(3)**, 341.

51. Quadri, T. W., Olasunkanmi, L. O., Fayemi, O. E., Solomon, M. M. and Ebenso, E. E. (2017) Zinc oxide nanocomposites of selected polymers: synthesis, characterization, and corrosion inhibition studies on mild steel in HCl solution. *ACS Omega*, **2(11)**, 8421–8437.

52. Senturk Parreidt, T., Lindner, M., Rothkopf, I., Schmid, M. and Müller, K. (2019) The development of a uniform alginate-based coating for cantaloupe and strawberries and the characterization of water barrier properties. *Foods*, **8(6)**, 203.